

Identification of Glycan Structure Alterations on Cell Membrane Proteins in Desoxyepothilone B Resistant Leukemia Cells^{*S}

Miyako Nakano^{‡||}, Rohit Saldanha[§], Anja Göbel[§], Maria Kavallaris^{§¶||‡‡},
and Nicolle H. Packer^{‡**‡‡}

Resistance to tubulin-binding agents used in cancer is often multifactorial and can include changes in drug accumulation and modified expression of tubulin isotypes. Glycans on cell membrane proteins play important roles in many cellular processes such as recognition and apoptosis, and this study investigated whether changes to the glycan structures on cell membrane proteins occur when cells become resistant to drugs. Specifically, we investigated the alteration of glycan structures on the cell membrane proteins of human T-cell acute lymphoblastic leukemia (CEM) cells that were selected for resistance to desoxyepothilone B (CEM/dEpoB). The glycan profile of the cell membrane glycoproteins was obtained by sequential release of *N*- and *O*-glycans from cell membrane fraction dotted onto polyvinylidene difluoride membrane with PNGase F and β -elimination respectively. The released glycan alditols were analyzed by liquid chromatography (graphitized carbon)-electrospray ionization tandem MS. The major *N*-glycan on CEM cell was the core fucosylated α 2-6 monosialo-biantennary structure. Resistant CEM/dEpoB cells had a significant decrease of α 2-6 linked sialic acid on *N*-glycans. The lower α 2-6 sialylation was caused by a decrease in activity of β -galactoside α 2-6 sialyltransferase (ST6Gal), and decreased expression of the mRNA. It is clear that the membrane glycosylation of leukemia cells changes during acquired resistance to dEpoB drugs and that this change occurs globally on all cell membrane glycoproteins. This is the first identification of a specific glycan modification on the surface of drug resistant cells and the mechanism of this downstream effect on microtubule targeting drugs may offer a route to new interventions to overcome drug resistance. *Molecular & Cellular Proteomics* 10: 10.1074/mcp.M111.009001, 1–12, 2011.

From the [‡]Department of Chemistry and Biomolecular Sciences, Macquarie University, NSW 2109, Australia; [§]Children's Cancer Institute Australia, Lowy Cancer Research Centre, UNSW, Randwick, NSW 2031, Australia; [¶]Australian Centre for Nanomedicine, UNSW, Sydney, 2052, Australia; ^{||}Graduate School of Advanced Sciences of Matter, Hiroshima University, Hiroshima 739-8530, Japan

Received March 9, 2011, and in revised form, August 6, 2011

Published, MCP Papers in Press, August 22, 2011, DOI 10.1074/mcp.M111.009001

Epothilones are a promising class of tubulin-binding agent that stabilize microtubules against depolymerization and that have shown promising preclinical and clinical activity. An analog of epothilone B (Ixabepilone, BMS-247550, aza-EpoB) has been approved for the treatment of drug refractory metastatic breast cancer (1). Epothilones target β -tubulin on the α/β -tubulin heterodimer, inducing potent mitotic arrest and cell death (2, 3). Resistance to tubulin-binding agents such as the vinca alkaloids, taxanes, and epothilones has primarily been associated with the cellular target of the drug, tubulin mutations and altered expression of specific tubulin isotypes (4). We have previously described the selection and characterization of T-cell acute lymphoblastic leukemia cells selected for resistance to an epothilone B analog, Z12, 13-desoxyepothilone B (dEpoB)¹ (5, 6). These dEpoB resistant cells acquired multiple alterations associated with microtubules, including increased expression of β III-tubulin, increased expression of MAP4, and mutations in β I-tubulin (6).

It is well known that apoptosis plays a role in preventing cancer. If a cell is unable to undergo apoptosis because of a mutation or biochemical inhibition, it can continue to divide and develop into a tumor. It is also known that protein glycosylation changes with apoptosis in different biological systems. Recently, Malagolini *et al.* reported that expression of α 2-6 sialylated lactosamine chains resulted in apoptotic and necrotic death of cell lines from different histological origin, (colon, breast, pancreas, and bladder cancer) (7). Honma *et al.* reported a relationship between apoptosis and alteration of the glycosylation pathway in a human breast cancer cell line resistant to docetaxel, an agent that, like epothilone, stabilizes microtubules against depolymerization. In this study, regulation of the gene encoding ribophorin II (RPN2), which is part of the *N*-oligosaccharyl transferase complex, efficiently induced apoptosis of docetaxel-resistant human breast cancer cells (MCF7-ADR cells) in the presence of docetaxel. RPN2 silencing induced reduced glycosylation of the P-glycoprotein, as

¹ The abbreviations used are: dEpoB, Z12, 13-desoxyepothilone B; Hex, hexose; Glc, glucose; Gal, galactose; Man, mannose; Fuc, fucose; HexNAc, *N*-acetylhexosamine; GlcNAc, *N*-acetylglucosamine; GalNAc, *N*-acetylgalactosamine; NeuAc, *N*-acetylneuraminic acid; BPC, Base peak chromatogram; EIC, Extracted ion chromatogram.

well as decreased membrane localization, thereby sensitizing MCF7-ADR cells to docetaxel (8). These two reports focused on the relative alteration of glycan structures using lectin staining or gel migration changes on SDS-PAGE, but did not identify the actual glycan structures associated with these drug resistance mechanisms.

Glycans on glycoproteins are classified into two types; *N*-glycan (attached to the Asn residue in the Asn-X-Ser/Thr sequon) and *O*-glycan (attached to Ser/Thr residues). All *N*-glycans have a common core structure, Man α 1-6(Man α 1-3)Man β 1-4GlcNAc β 1-4GlcNAc β 1-, and are classified into three types: (1) high-mannose type, in which only Man residues are attached to both of the Man α 1-6 and Man α 1-3 arms of the core structure; (2) hybrid type, in which Man residues are attached to only the Man α 1-6 arm, an “antennae” structure produced through the action of *N*-acetylglucosaminyltransferases being attached to the Man α 1-3 arm; and (3) complex type, in which the “antennae” structure is attached to both the Man α 1-6 and Man α 1-3 arms.

Detailed analysis of changes in glycan structures can be used to identify the specific enzyme(s) or gene(s) involved in glycosylation-related pathways involved in drug resistance mechanisms. This paper describes the alterations to glycan structures on cell membrane proteins of CEM cells with acquired resistance to dEpoB that were not present in the parental drug sensitive CEM cells. Thus, alterations to the glycans attached to cell membrane proteins may contribute to the phenotype associated with dEpoB resistance.

EXPERIMENTAL PROCEDURES

Materials—*N*-Glycosidase F (PNGase F, EC 3.5.1.52, recombinant cloned from *Flavobacterium meningosepticum* and expressed in *E. coli*) was purchased from Roche Diagnostics (Mannheim, Germany). Alpha2-3 sialidase was from Takara Bio (Shiga, Japan). Alpha2-3,6 sialidase, α 2-3,6,8,9 sialidase and α 1-3/4 fucosidase were from Northstar bioproducts (East Falmouth, MA). Beta1-4 galactosidase was from ProGlycAn (Wien, Austria). Polyvinylidene difluoride (PVDF) (0.2 μ m, for sequencing, 7 \times 8.4 cm) was purchased from Bio-Rad (Hercules, CA). Cation-exchange columns were made of (30 mg) Dowex 50W-X8 resin (Supelco, Bellefonte, PA) packed on top of a 10 μ l ZipTip of reversed phase μ C₈ (Millipore, Billerica, MA). The resins were protonated with 1 M HCl (50 μ l, 3 times), were washed with methanol (50 μ l, 3 times), and then equilibrated with water (50 μ l, 3 times) before use. Microtiter plates (96-well flat bottom) were purchased from Costar. Premade SDS-PAGE gels (4–12% (w/v), Tris-Glycine, 12-well), LDS buffer (40% (v/v) glycerol, 4% (w/v) lithium dodecyl sulfate, 0.8 M triethanolamine-Cl (pH 7.6), 4% (w/v) Ficoll 400, 0.025% (w/v) Phenol Red, 0.025% (w/v) Brilliant blue G250 and 2 mM EDTA) and running buffer (SDS Run Buffer x20) were purchased from PAGEgel INC (San Diego, CA). All other chemicals were purchased from Sigma-Aldrich. Other reagents and solvents were of HPLC or LC/MS grade.

Cell Culture and Preparation of Resistant Cells—A human T-cell acute lymphoblastic leukemia cell line, CCRF-CEM (CEM), was maintained in RPMI 1640 containing 10% (w/v) fetal calf serum as suspension cultures. CEM cells were previously selected by multiple stepwise treatments with increasing concentrations of dEpoB (6). The resulting cell lines have since been maintained in drug-free media and are routinely screened and free of mycoplasma. Cells

were grown to mid-log phase, collected by centrifugation at 1000 rpm and washed with phosphate-buffered saline (PBS) three times, and cell pellets were stored at -80°C before glycan analysis.

Cell Membrane Preparation—Cell pellets (1×10^7 cells) were homogenized in 2 ml of lysis buffer containing 50 mM Tris-HCl (pH 7.4), 0.1 M NaCl, 1 mM EDTA, and protease inhibitor mixture (Roche Diagnostics, Mannheim, Germany) using a polytron homogenizer (Omni TH homogenizer, Omni International, Inc., VA; 15 s, 7 times on ice bath). We performed the following preparation according to the procedure reported by Lee *et al.* (9) with some modifications. The homogenized cells were centrifuged at $2000 \times g$ for 20 min at 4°C to precipitate nuclei and unlyse cells. The supernatant was diluted with 2 ml of Tris-buffer (20 mM Tris-HCl (pH 7.4), 0.1 M NaCl) and then were sedimented by ultracentrifugation at $120000 \times g$ for 80 min at 4°C . The supernatant was discarded, and the membrane pellet was suspended in 100 μ l Tris-buffer. After adding 400 μ l Tris-buffer containing 1% (v/v) Triton X-114, the suspended mixture was homogenized by pipeting strongly (9–11). The homogenate was chilled on ice for 10 min and incubated at 37°C for 20 min and then phase partitioned by centrifugation at $1000 \times g$ for 3 min. The upper aqueous phase was removed. The lower detergent phase was further mixed with 1 ml of ice-cold acetone and kept at -25°C overnight to precipitate proteins and remove any detergent. After centrifugation at $1000 \times g$ for 3 min, the precipitated cell membrane proteins were stored at -25°C if not used immediately.

Enzymatic Release and Purification of *N*-glycans from Cell Membrane Proteins—The precipitated membrane proteins were dissolved with 10 μ l 8 M Urea. The solubilized proteins were dotted (2.5 μ l \times 4 times) onto polyvinylidene difluoride (PVDF) membrane prewetted with ethanol. After drying the PVDF membrane at room temperature overnight, the PVDF membrane was washed with ethanol for 1 min and then washed three times for 1 min with water. The protein on the membrane was stained for 5 min with Direct Blue 71 (800 μ l solution A: 0.1% (w/v) Direct Blue 71 (Sigma-Aldrich) in 10 ml solution B: acetic acid : ethanol : water = 1:4:5). After destaining with solution B for 1 min, the PVDF membrane was dried at room temperature for 4 h. *N*- and *O*-glycans were released from the dotblotted proteins essentially by the method of Wilson *et al.* (12) with some modifications. Protein stained blue were cut from the PVDF membrane and placed in separate wells of a 96-well microtiter plate. The spots were then covered with 100 μ l of 1% (w/v) poly(vinylpyrrolidone) 40000 in 50% (v/v) methanol, agitated for 20 min, and washed with water (100 μ l \times 5 times). PNGase F (3U in 10 μ l of 30 mM phosphate buffer (pH 7.3)) was added to each well and incubated at 37°C for 15 min. An additional 10 μ l of water was added to each well and incubated at 37°C overnight to release *N*-glycans. During the incubation, the sample wells were sealed with amplification tape to prevent evaporation. To collect the released *N*-glycans, the samples were sonicated (in the 96-well plate) for 10 min, and the released *N*-glycans (20 μ l) were transferred to 1.5-ml polypropylene tubes. The sample well was washed with water (50 μ l twice), and the washings combined. To completely generate the reducing terminus, ammonium acetate buffer (100 mM, pH 5.0, 20 μ l) was added to the released *N*-glycans for 1 h at room temperature. After evaporating to dryness, the glycans were reduced with 20 μ l of 1 M NaBH₄ in 50 mM KOH at 50°C for 3 h. One microliter of acetic acid was added to stop the reaction, and the *N*-glycan alditols were desalted using a cation-exchange column. The glycan alditols were eluted with water (50 μ l twice), dried, and the remaining borate was removed by the addition of (100 μ l \times 3) methanol and drying under vacuum. The glycan alditols were resuspended in 10 mM NH₄HCO₃ (20 μ l) immediately before glycan analysis by liquid chromatography-electrospray ionization mass spectrometry (LC-ESI MS).

Chemical Release and Purification of *O*-glycans from Cell Membrane Proteins—After the removal of the *N*-glycans, each protein spot

remaining on the membrane was rewet with 2.5 μl of methanol. A solution of 0.5 M NaBH_4 in 50 mM KOH (20 μl) was applied, and the spots were incubated for 16 h at 50 °C in order to release O-glycan alditols. After adding 2 μl of acetic acid to stop the reaction, the same procedures as for the clean up of N-glycan alditols was used.

LC-ESI MS for Analysis of Glycan Alditols—Both N- and O-glycan alditols were separated using a HyperCarb porous graphitized carbon column (5 μm HyperCarb, 300 μm I.D. \times 100 mm, Thermo Hypersil, Runcorn, UK) under the following gradient conditions. The separation of N-glycans was performed using a sequence of isocratic and two segmented linear gradients: 0–8 min, 10 mM NH_4HCO_3 ; 8–53 min, 6.75–15.75% (v/v) CH_3CN in 10 mM NH_4HCO_3 ; 53–73 min, 15.75–40.5% (v/v) CH_3CN in 10 mM NH_4HCO_3 ; and increasing to 81% (v/v) CH_3CN in 10 mM NH_4HCO_3 for 6 min and re-equilibrated with 10 mM NH_4HCO_3 for 4 min. The separation of O-glycans was performed with an isocratic and two segmented linear gradients: 0–8 min, 10 mM NH_4HCO_3 ; 8–33 min, 0–22.5% (v/v) CH_3CN in 10 mM NH_4HCO_3 ; 33–37 min, 22.5–40.5% (v/v) CH_3CN in 10 mM NH_4HCO_3 ; and increasing to 81% (v/v) CH_3CN in 10 mM NH_4HCO_3 for 6 min and re-equilibrated with 10 mM NH_4HCO_3 for 4 min. The HPLC flow rate was 500 $\mu\text{l}/\text{min}$ with a split ratio of 1/100 to give a final flow rate of 5 $\mu\text{l}/\text{min}$ through the column (UltiMate 3000, Dionex, USA). The injection volume of samples was 5 μl . In the MS (Esquire HCT, Bruker Daltonics GmbH, Bremen, Germany), the voltage of the capillary outlet was set at 3 kV, and the temperature of the transfer capillary was maintained at 300 °C. The flow rate of nitrogen gas for drying was 6 L/min. The MS spectra were obtained in the negative ion mode over the mass range m/z 100 to m/z 2500. The scan rates were 8100 amu/s for the MS mode and the MS/MS mode. Monoisotopic masses were assigned with possible monosaccharide compositions using the GlycoMod tool available on the ExPASy server (<http://au.expasy.org/tools/glycomod>; mass tolerance for precursor ions is \pm 0.1 Da) and the proposed oligosaccharide structures were further verified through annotation using a fragmentation mass matching approach based on the MS/MS data. Validation of the technical reproducibility of the analytical conditions such as retention time and mass number was carried out using known glycans derived from fetuin (supplemental Fig. S1), before analyzing any experimental samples.

The Relative Abundance of N-glycan and O-glycan Structures on Cell Membrane Glycoprotein of CEM and CEM/dEpoB Cells—The relative abundance of each glycan structure on the cell membrane glycoproteins of CEM and drug-resistant cells was calculated based on the peak area of the extracted ion chromatogram (EIC) of the corresponding glycan structure, after processing of the peaks (smoothing algorithm; Gauss, smoothing widths; 3 pnts (for N-glycan) or 1 pnts (for O-glycan) using Bruker Daltonics DataAnalysis software version 3.4. The peak areas of all the glycan structures released from each sample was summed and set to 100%, and the relative abundance (%) was calculated for each glycan structure.

Specific Sialidase Digestions of Glycan Samples—N- and O-glycan samples were digested with three different sialidases to determine the specific linkage of sialic acid. Three portions (1 μl , 0.5 μl , and 0.5 μl) of the N-glycan alditols were mixed with 250 mM ammonium acetate (pH 6.0, 2 μl), and made up to 9 μl with water respectively. Alpha2–3 sialidase (50 mU, 1 μl), α 2–3,6 sialidase (15 mU, 1 μl), and α 2–3,6,8,9 sialidase (5 mU, 1 μl) were added to the mixtures respectively and incubated at 37 °C overnight. After heating at 99 °C for 2 min to stop the reaction, each digest was analyzed by LC-EIS MS.

Specific Fucosidase and Galactosidase Digestions of Glycan Samples—Desialylated N-glycan samples were digested with α 1–3,4 fucosidase and β 1–4 galactosidase for further structural information. N-glycan alditols (1 μl) were desialylated by incubating with 100 μl of 2 M acetic acid at 80 °C for 2 h and were evaporated to dryness. The residue was dissolved in 50 mM ammonium acetate (pH 6.0, 30 μl)

and was equally divided into three equal portions. One portion of the sample was injected to LC-ESI MS to confirm whether the glycans had been fully desialylated and the other two portions of the sample was digested with α 1–3,4 fucosidase (0.5 mU, 1 μl) and β 1–4 galactosidase (0.3 mU, 1 μl), respectively, at 37 °C for 1 h. After stopping the reaction at 99 °C for 2 min, each digested sample was analyzed by LC-EIS MS and compared with the original structures.

Analysis of Glycans on Glycoproteins Separated on SDS-PAGE—Cell membranes from 4×10^7 cells were prepared as above and the acetone-precipitated proteins were dissolved in water (13 μl), 500 mM dithiothreitol (2 μl) and LDS buffer (5 μl), heated at 70 °C for 10 min, and 10 μl was separated by SDS-PAGE. After the electrophoresis, proteins were transferred to PVDF membrane under semiwet conditions by means of a Novex Mini-Cell (Invitrogen) in transfer buffer (0.1 M Glycine, 0.012 M Tris, and 20% (v/v) methanol). The PVDF membrane was washed three times with water for 1 min each. The proteins on PVDF membrane were stained with Direct Blue 71. After destaining, the PVDF membrane was dried at room temperature for 4 h and the protein bands cut into pieces (0.5 \times 0.5 cm), combined together as five different molecular weight range fractions (<35 kDa, 35–55 kDa, 55–85 kDa, 85–200 kDa, and >200 kDa) in separate wells of a 96-well microtiter plate, and the N-glycans released and analyzed as above.

Measurement of ST6Gal Enzyme Activity with 2-Aminopyridine (PA)-labeled N-glycan as Acceptor—The measurement of the activity of ST6Gal was performed by an adaptation of the method of Dall'Olio *et al.* (13). Their method is based on the enzyme-catalyzed transfer of radioactive sialic acid from the donor substrate (CMP-[^{14}C]NeuAc) to an acceptor that is an asialo-glycan. In this study we used the fluorescently PA-labeled biantennary asialo-N-glycan (Takara bio, Shiga, Japan) as acceptor and unlabeled CMP-NeuAc (Calbiochem, La Jolla, CA) as donor substrate. Cells (1×10^7) were homogenized by vigorous pipeting up and down (50 times) in 40 μl of ice-cold water. To the homogenized solution, 4 μl of 1 M sodium cacodylate (pH 6.5), 2.5 μl of 10% Triton X-100, 2 μl of PA-labeled biantennary asialo-N-glycan (20 pmol), and 1 μl of CMP-NeuAc (1.5 nmol) were added and the mixture was incubated at 37 °C overnight. Water (2 μl) was added instead of the acceptor as a control. After incubation, water (100.5 μl) was added to the reaction mixture, and the mixture was filtered through a 10 kDa molecular weight cutoff membrane filter (Nanosep, PALL life sciences, Port Washington, NY) using centrifugation (12000 $\times g$, 10 min). The retentate on the membrane was washed with 50 μl of water, and the washing combined to give a resulting total volume of 200 μl . A portion (10 μl) of the solution was separated by normal phase HPLC with a Shimadzu 10A HPLC system equipped with a fluorescence detector (Shimadzu RF-10AXL). Separation was carried out at a flow rate of 0.2 ml/min at 50 °C using a polymer-based Asahi Shodex NH2P-50 2D column (Showa Denko, Tokyo, Japan; 2 \times 150 mm) with a linear gradient formed by 2% acetic acid in acetonitrile (solvent A) and 5% acetic acid in water containing 3% triethylamine (solvent B). The column was initially equilibrated and eluted with 20% solvent B for 2 min, at which point the concentration of solvent B was increased to 80% over 60 min. Next the column was washed with 95% solvent B for 15 min and equilibrated with 20% solvent B for 25 min. The PA-labeled acceptor (biantennary asialo-N-glycan) and product (biantennary sialo-N-glycans), were measured by fluorescence detection at $\lambda_{\text{ex}} = 320$ nm and $\lambda_{\text{em}} = 400$ nm.

LC-ESI MS of PA-labeled Glycans—PA-labeled N-glycans were collected from the HPLC analysis and were analyzed by LC-ESI MS in order to identify the linkage and the position of the sialic acid added to the acceptor glycan. The analytical conditions were the same as LC-ESI MS for analysis of N-glycan alditols with a different separation gradient: a sequence of an isocratic and two segmented linear gradients: 0–8 min, 10 mM NH_4HCO_3 ; 8–65 min, 2.25–22.5% CH_3CN in

10 mM NH_4HCO_3 ; 65–73 min, 22.5–45% CH_3CN in 10 mM NH_4HCO_3 ; and then stepping up to 81% CH_3CN in 10 mM NH_4HCO_3 which was kept for 6 min (to clean the column) and back to 10 mM NH_4HCO_3 for 4 min (to re-equilibrate) was used.

Cell Staining with Fluorescently Labeled Lectins—Cultured cells (2×10^6) were washed twice with 1 ml of cold PBS using centrifugation ($370 \times g$, 7 min, 4°C). The cell pellet was mixed with biotin conjugated *Sambucus sieboldiana* (SSA) lectin ($1 \mu\text{g}$ in $50 \mu\text{l}$ of PBS, J-OIL MILLS, INC., Tokyo, Japan) or biotin conjugated *Maackia amurensis* (MAM) lectin ($1 \mu\text{g}$ in $50 \mu\text{l}$ of PBS, J-OIL MILLS, INC., Tokyo, Japan), and kept on ice for 30 min. After washing with cold PBS using centrifugation ($370 \times g$, 7 min, 4°C), the cell pellet was mixed with streptavidin conjugated R-phycoerythrin-cyanine dye (PE-Cy7) ($0.5 \mu\text{g}$ in $50 \mu\text{l}$ of PBS, BD Biosciences) and kept on ice for 30 min. After washing with cold PBS using centrifugation ($370 \times g$, 7 min, 4°C) three times, the cell pellet was suspended by vigorous pipetting up and down (35 times) in $20 \mu\text{l}$ of cold PBS. All samples were observed using a Nikon Eclipse E600 fluorescence microscope (Tokyo, Japan).

Quantitative Real Time RT-PCR of ST6GAL-I—Cells were harvested during their mid-log cellular growth phase of 5×10^5 – 1×10^6 cells/ml and cell pellets were frozen and stored at -80°C until required for RNA isolation. RNA isolation was performed using the RNeasy Plus Mini Kit (Qiagen) according to manufacturer's instructions. RNA concentration was determined using the NanoDrop® ND-1000 spectrophotometer. Two hundred nanogram of RNA was reverse transcribed in a total volume of $10 \mu\text{l}$. Quantitative Real Time RT-PCR (qRT-PCR) was performed to determine the relative gene expression of ST6GAL-I in the CEM and CEM/dEpoB300 cells. PCR reactions were carried out using $1 \mu\text{l}$ of cDNA, $2 \times$ TaqMan Gene Expression Master mix, $20 \times$ ST6GAL-I TaqMan Gene Expression (Applied Biosystems, assay ID Hs00949382), and two independent housekeeping genes, human *Cyclophilin A* (*PPIA*) and human *large ribosomal protein* (*RPLPO*) (Applied Biosystems) were used as control genes. Conditions for the qRT-PCR on the ABI Prism 7900 HT (Applied Biosystems) were 2 min at 50°C , followed by 40 cycles of denaturation for 10 min at 95°C , annealing and extension for 1 min at 60°C . Data analysis was performed using the SDS 2.3 Software (Applied Biosystems) and the relative gene expression of ST6GAL-I was calculated using the $\Delta\Delta\text{CT}$ method, formula = $(2^{-\Delta\Delta\text{CT}})$, $\Delta\Delta\text{CT} = \Delta\text{CT}(\text{CEM/dEpoB300}) - \Delta\text{CT}(\text{CEM})$ where $\Delta\text{CT} = \text{average CT value of the gene of interest (ST6GAL-I)} - \text{average CT value of the control gene (PPIA/RPLPO)}$. Data represent three individual experiments performed in triplicate.

RESULTS

Characterization of Glycan Structures on Membrane Proteins of CEM and CEM/dEpoB Resistant Leukemia Cells—*N*-Glycans were released from cell membrane glycoproteins by PNGase F and were analyzed by LC-ESI MS and MS/MS as *N*-glycan alditols. The base peak chromatograms (BPC) of the separated *N*-glycans (Fig. 1A–1C) showed that the global profile of the glycan structures on the cell membrane glycoproteins of CEM cells were different from that of CEM cells selected for resistance to 30 nM dEpo30 (CEM/dEpoB30) and 300 nM dEpoB (CEM/dEpoB300). The numbers attached to each peak in Fig. 1 correspond to the identification of 20 glycan masses comprising 47 different *N*-glycan structures as summarized in Fig. 2. These structures included high mannose type *N*-glycans (structures #1–5), asialo-*N*-glycans (structures #6–10), monosialo-*N*-glycans (structures #11, 12, 15, 16), disialo-*N*-glycans (structures # 13, 14, 17), trisialo-*N*-

glycans (structures # 18, 19), and a tetrasialo-*N*-glycan (structure # 20) with and without fucosylation and with different sialylation linkages and positions. The relative abundances (%) of each glycan structure on the cell membrane glycoproteins of the three cell lines are shown in Fig. 2. This was calculated by setting the total peak area of glycans in each BPC as 100%, and the relative abundance (%) was calculated using the area under the EIC peak for each glycan structure. High mannose type *N*-glycans, (structures # 1 + 2+3 + 4+5) in CEM cell, CEM/dEpoB30, and CEM/dEpoB300, were observed in large amounts in all three cell lines and comprised 34.3%, 40.7%, and 36.6% of the total glycan structures on the cell membrane glycoproteins respectively.

Fucosylated monosialo-*N*-glycans (structure # 12, $1038.9 m/z$ [$\text{M}-2\text{H}$] $^{2-}$) were observed as the major complex type *N*-glycans on all cells with a different distribution of isomers. This *N*-glycan composition (structure # 12) presents as four structural isomers with different retention times; #12a (42 min), #12b (44 min), #12c (54 min), and #12d (55 min) in the BPC in Fig. 1A–C. Fucosylated disialo-*N*-glycans (structure # 14, $1184.4 m/z$ [$\text{M}-2\text{H}$] $^{2-}$) were observed as the second major complex type *N*-glycans with a similar different distribution of isomers between the cell types. This *N*-glycan mass (structure #14) has three structural isomers; #14a (49 min), #14b (58 min), and #14c (60 min) that were separated by graphitized carbon column chromatography (Fig. 1A–1C).

To determine the exact structural differences between these isomers, specific sialidases were used to characterize the linkage of NeuAc to galactose (Gal). The total released *N*-glycans from the CEM cell glycoproteins (Fig. 3A) were treated with α 2-3 sialidase (Fig. 3B), α 2-3,6 sialidase (Fig. 3C), and α 2-3,6,8,9 sialidase (Fig. 3D), respectively. The EICs at $1184.4 m/z$ [fucosylated disialo-biantennary *N*-glycan (structure #14)], $1038.9 m/z$ [fucosylated monosialo-biantennary *N*-glycan (structure #12)] and the fully desialylated biantennary product mass at $893.3 m/z$ [fucosylated asialo-biantennary *N*-glycan (structure #7)] were chosen to monitor the effect of the sialidase digestions of these mono-sialylated and di-sialylated *N*-glycans. The structures #14b and #14c disappeared and the structures #12b and #7 increased after α 2-3 sialidase (Fig. 3B), indicating that the isomers consist of biantennary structures with one α 2-3 NeuAc and two α 2-3 NeuAc on the termini, whereas #12a, #12b, and #14a did not disappear, indicating that their structures do not contain terminal α 2-3 NeuAc. Structures #12c and #12d both moved to the retention time of structure #7 after α 2-3 sialidase digestion, indicating that these mono-sialylated structures are linked to α 2-3 NeuAc. After digestion with α 2-3,6 sialidase and α 2-3,6,8,9 (Fig. 3C and 3D), all structures were fully de-sialylated (to structure #7). In summary, *N*-glycan structures #12a, #12b, and #14a consist of NeuAc linked only as α 2-6, and #12c, 12d, and 14c consist of NeuAc linked only as α 2-3, and #14b consists of both α 2-3 NeuAc and α 2-6 NeuAc linkages.

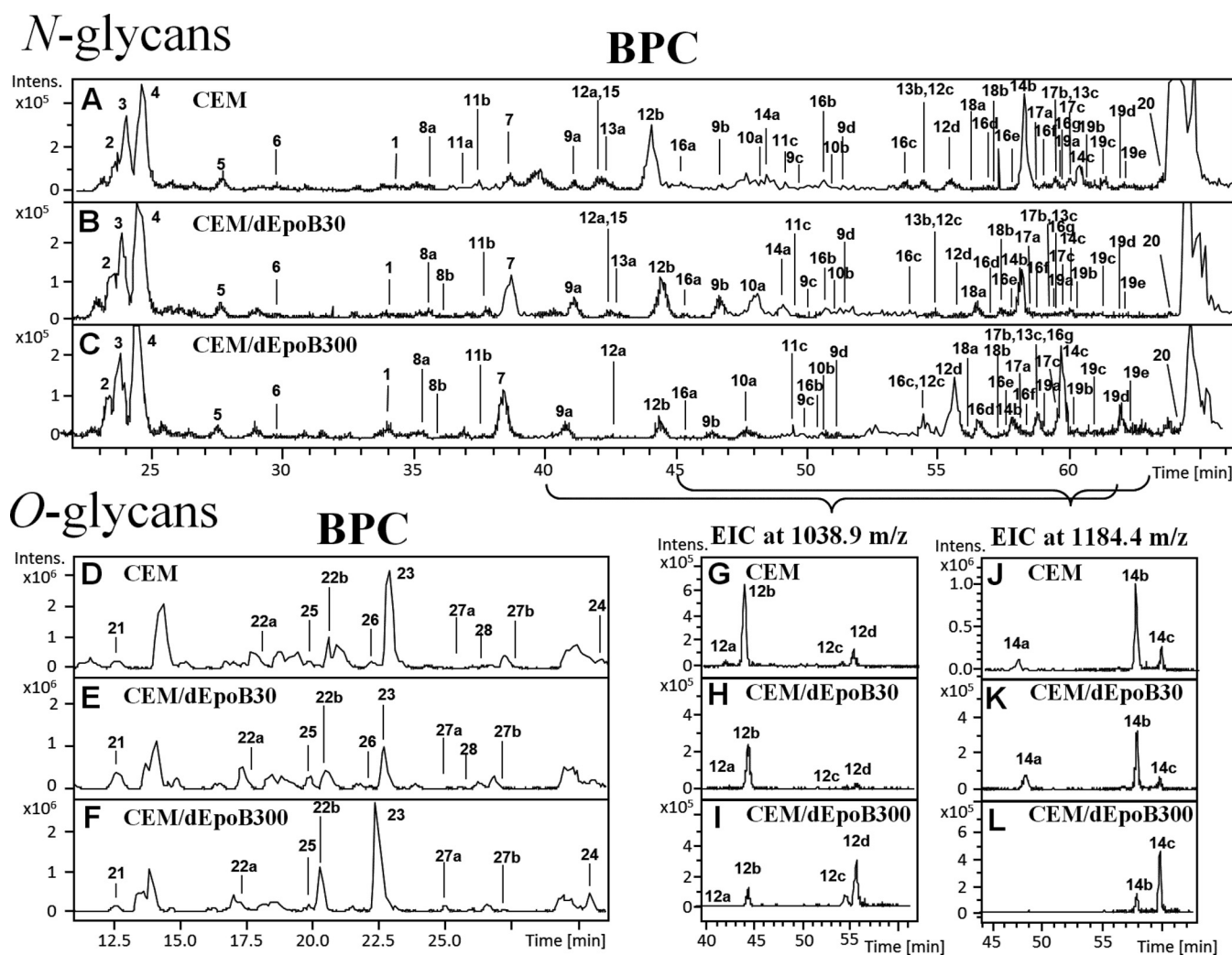


Fig. 1. LC-ESI MS analysis of *N*-glycans and *O*-glycans released from cell membrane glycoproteins. A–C; BPC for *N*-glycans from CEM cell (A), CEM/dEpoB30 cell (B) and CEM/dEpoB30 cell (C). D–F; BPC for *O*-glycans from CEM (D), CEM/dEpoB30 cell (E) and CEM/dEpoB30 cell (F). G–I: EIC at 1038.9 *m/z* for fucosylated monosialo-bi-antennary *N*-glycan (structure # 12), J–L: EIC at 1184.4 *m/z* for fucosylated disialo-bi-antennary *N*-glycan (structure # 14). The structures of *N*-glycans and *O*-glycans are shown in Fig. 2.

The linkage position of NeuAc on the mono-sialylated bi-antennary *N*-glycan structures #12a–d was also determined from their MS/MS spectra. For this determination, *N*-glycans of bovine fetuin, whose structures were already identified in detailed by Townsend *et al.* (14) and Green *et al.* (15), were analyzed by LC-ESI MS and MS/MS (supplemental Fig. S1) and used as standard structures for comparison. The fetuin bi-antennary and tri-antennary *N*-glycan isomers, which include sialic acids (NeuAc) attached with different linkages and positions were observed in the BPC (supplemental Fig. S1A). The EIC of the monosialo-bi-antennary *N*-glycans (structure # 11, 965.8 *m/z* [M–2H]^{2–}) (16) showed the presence of 4 isomers (supplemental Fig. S1B), and each isomeric ion was subjected to MS/MS analysis. We found a diagnostic ion in the MS/MS spectra which was able to distinguish the sialylated mannose branch of the monosialo-bi-antennary *N*-glycans. If NeuAc is located on the α 1–6 Man branch of this

structure, a fragment ion at 979.3 *m/z*, which corresponds to the mass of [NeuAc–Gal–GlcNAc–Man– α 1–6 Man], was observed (supplemental Fig. 2A and 2C), whereas this fragment is not seen in the MS/MS spectrum if NeuAc is located on the α 1–3 Man branch (supplemental Fig. 2B and 2D).

N-glycan structural isomers #12a–d released from the CEM cell glycoproteins (as shown in Fig. 3A) were subjected to MS/MS analysis, and this diagnostic ion fragment ion of 979.3 *m/z* was not observed in the MS/MS spectra of *N*-glycan structures #12b and 12d (Figs. 3E and 3F) but was observed in MS/MS fragmentation spectra of *N*-glycan structures #12a and 12c (data not shown). Thus it can be deduced that the mono-sialylated bi-antennary *N*-glycan structures #12a and #12c are sialylated on the α 1–6 Man branch whereas structures #12b and #12d have NeuAc on the α 1–3 Man branch.

The linkage of fucose (Fuc) on the *N*-glycans was characterized using specific fucosidase and galactosidase diges-

tions. The results of digestions of the disialo-bi-antennary *N*-glycan with one Fuc (structure #14) and trisialo-tri-antennary *N*-glycan with one Fuc (structure #19) are shown in [supplemental Fig. S3](#) and [supplemental Fig. S4](#), respectively. Using α 1–3,4 fucosidase after desialylation with mild acid did not result in a change in retention or mass of the desialylated structures. In addition, β 1–4 galactosidase resulted in removal of the mass of galactose; because this enzyme can only remove terminal galactose if it is not fucosylated, it was deduced that the Fuc on the biantennary and triantennary *N*-glycans is α 1–6 linked core fucose. Bi-antennary *N*-glycans with two Fuc (structure #8 and #15) were also observed in this study. After digestion with α 1–3,4 fucosidase, the bi-antennary *N*-glycan with two Fuc (structure #8) was no longer observed. After further digestion with β 1–4 galactosidase, the bi-antennary *N*-glycan lost one Gal (structure #33 in [supplemental Fig. S3D](#)). These results showed the linkages of Fuc on the biantennary *N*-glycans (structure #8 and #15) were α 1–6 (core Fuc) and α 1–3,4 (Lewis^{x/a} Fuc). Sialylated fucosylated tetra-antennary *N*-glycans (structure #20) were also observed, but the linkage of Fuc could not be identified as they were in low abundance (CEM; 0.09%, CEM/dEpoB30; 0.04%, CEM/dEpoB300; 0.14%). The detailed *N*-glycan structures found in CEM cell, CEM/dEpoB30 cell, and CEM/dEpoB300 cell were characterized in this way and are shown in Fig. 2.

Thus we show that high mannose *N*-glycans comprise the major structures in all the cell lines, but that the major complex type core fucosylated monosialo-biantennary *N*-glycans in CEM and CEM/dEpoB30 cells are α 2–6 NeuAc sialylated (structure #12b, 10.3%, and 7.0%, respectively), whereas the *N*-glycans of the drug resistant CEM/dEpoB300 cells are sialylated with α 2–3 NeuAc linkage (structure #12d, 7.2%). In addition, the α 2–3 NeuAc sialylation of the core fucosylated disialo-biantennary *N*-glycans increases markedly in the drug resistant CEM/dEpoB300 cells (structure #14c, 6.0%) relative to the control CEM cells. It is clear from this analysis that the *N*-glycans on the membrane glycoproteins of leukemia cells change with acquired resistance to dEpoB and that this change is related to different sialylation of the *N*-glycans.

O-Glycans were released by chemical β -elimination from the same cell membrane glycoproteins after the enzymatic release of *N*-glycans and were also analyzed by LC-ESI MS and MS/MS as O-glycan alditols. The BPC in Figs. 1D–1F showed that the chromatographic profile of O-glycan structures on the cell membrane glycoproteins of CEM, CEM/

dEpo30, and CEM/dEpoB300 cells were similar. For identification of O-glycan structures, O-glycans of bovine fetuin, whose structures have already been identified in detail by Karlsson *et al.* (17) and Royle *et al.* (18), were analyzed by LC-ESI MS and used as standard structures for comparison of retention time and fragmentation spectra. Specific sialidases were also used to characterize the linkage of NeuAc to Gal on the O-glycans of the CEM, CEM/dEpo30, and CEM/dEpoB300 cell membrane glycoproteins (data not shown). The ten O-linked structures identified are shown in Fig. 2, including a low abundance sulfated O-glycan (structure #26). Sialylation linked to Gal residue appears to be all α 2–3 NeuAc with some increased desialylation present in the dEpoB30 mildly resistant cells (structure #21 and #25, CEM/dEpo30) (Fig. 2).

Relative Quantification of Sialylated Glycan Isomers on Membrane Glycoproteins of CEM and dEpoB Resistant Leukemia Cells—EIC areas were used for comparison of the relative amount of the different sialoforms of bi-antennary *N*-glycan, tri-antennary *N*-glycan, and tetra-antennary *N*-glycan structures with and without fucose in CEM, CEM/dEpoB30, and CEM/dEpoB300 cells. The EIC of 1038.9 *m/z* [core fucosylated monosialo-bi-antennary *N*-glycan (structure #12)] in Fig. 1G–1I shows that an isomer with a NeuAc in α 2–3 linkage (structure #12d) is most abundant in CEM/dEpoB300 compared with both CEM and CEM/dEpoB30 cells. Also the EIC of 1184.4 *m/z* [core fucosylated disialo-bi-antennary *N*-glycan (structure #14)] in Fig. 1J–1L shows that an isomer with both NeuAc additions in an α 2–3 linkage (structure #14c) is most abundant in CEM/dEpoB300 cells. Other sialylated isomers are also seen to change in dEpoB300 cells; EIC of 1111.4 *m/z* [disialo-bi-antennary *N*-glycan (structure #13); [supplemental Fig 5A–C](#)] shows an increased isomer where both NeuAc are α 2–3 linked (structure #13c) and, although the exact linkage and the position of NeuAc on the fucosylated disialo-tri-antennary *N*-glycan (EIC of 1367.0 *m/z*) could not be characterized, the typically later elution position of α 2–3 NeuAc linked isomers off the carbon column indicates that the more abundant structure #17c ([supplemental Fig. 5D–F](#)) has two α 2–3 NeuAc. This difference in sialylation was not apparent in the less resistant dEpoB30 cells. Cells selected for resistance to 60 nM dEpoB (CEM/dEpoB60) or 140 nM dEpoB (CEM/dEpoB140) also did not show a significant change in NeuAc linkage [(structure #14) in [supplemental Fig. 6](#)]. These results demonstrate clearly that α 2–3 linked NeuAc is the dominant linkage on all *N*-glycans in the highest resistant cells, CEM/dEpoB300, compared with the CEM cells from

FIG. 2. **Bar graph of relative quantification of *N*-glycans and O-glycans observed in this study.** Symbols of monosaccharides and sulfonic residue (HSO₃) are shown in the panel at the lower right hand side. The number in parenthesis is mass numbers represented as [M–2H]^{2–} of alditol *N*-glycans and [M–H][–] of alditol O-glycans. The relative abundance (%) was calculated based on the peak area of EIC corresponding to glycans obtained from the results presented in Fig. 1. The error bar represents the standard deviation (S.D.) calculated from each type of cell (*n* = 3). To compare three groups [CEM, CEM/dEpoB30 and CEM/dEpoB300] repeated measures ANOVA (two-tail) was used, and then each groups of two was compared by Bonferroni correction (two-tail). The annotations in this figure indicate *p* < 0.01.

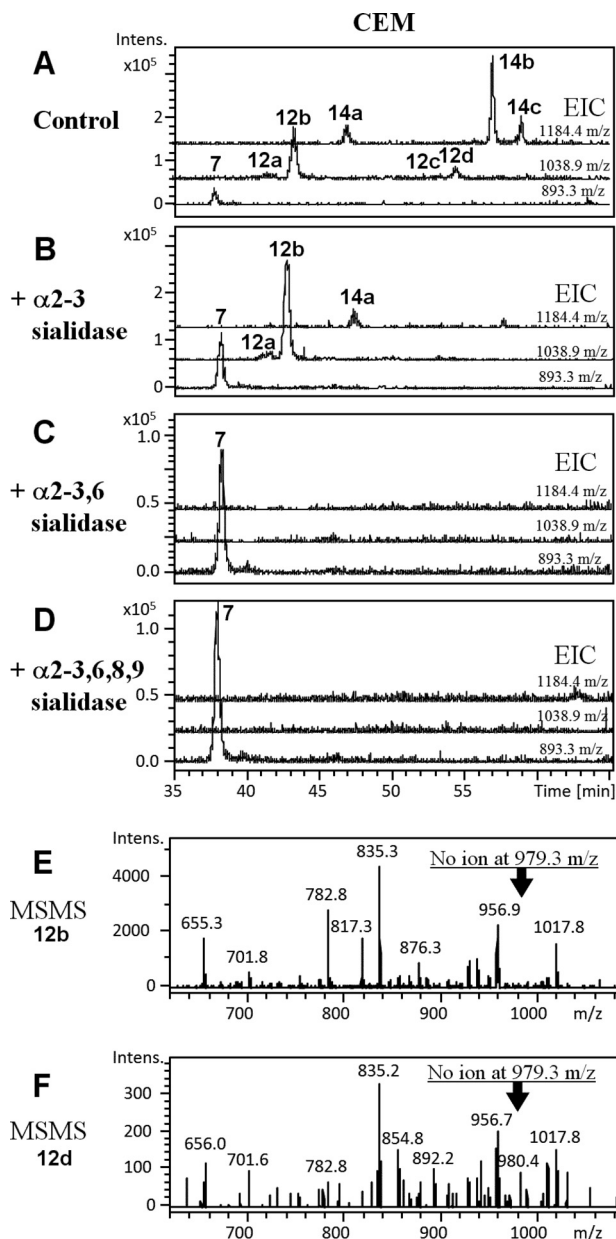


FIG. 3. Characterization of the linkage and position of sialic acids on fucosylated monosialo-bi-antennary *N*-glycans (structure # 12) and fucosylated disialo-bi-antennary *N*-glycans (structure # 14) on membrane glycoproteins of CEM cells using 3 kinds of specific sialidase and MS/MS. A–D: EIC at 1184.4 *m/z* for fucosylated disialo-biantennary *N*-glycan (structure # 14), EIC at 1038.9 *m/z* for fucosylated monosialo-biantennary *N*-glycan (structure # 12), EIC at 893.3 *m/z* for fucosylated asialo-biantennary *N*-glycan (structure # 7) before sialidase (A), after α 2-3 sialidase (B), after α 2-3,6 sialidase (C), and after α 2-3,6,8,9 sialidase (D). E and F: MS/MS analysis of two isomers of fucosylated monosialo-bi-antennary *N*-glycans (structures # 12b and 12d) observed in Fig. 3A, respectively.

which they are derived, and that the α 2-6 NeuAc linkage has been globally reduced on all *N*-glycan structures on the cell membrane proteins.

We also analyzed the O-glycans on the membrane glycoproteins of CEM, CEM/dEpoB30 and CEM/dEpoB300 cells. The EIC of the major sialylated O-glycan isomers of 675.2 *m/z* (supplemental Fig. 5G–I) showed no difference in these cells and there was also no alteration of the sialylation of the O-glycans in CEM/dEpoB60 and dEpoB140 resistant cells (data not shown). However, we did find an O-glycan structure that was not present only in the CEM/dEpoB 300 cells, which was identified as having the composition of a sulfated (HexNAc)₂(Hex)₂ (structure #26, supplemental Fig. 5J–L). There are three possible structures for this sulfated O-tetra-saccharide [(i)–(iii), supplemental Fig. 5M). The possible structures with sulfate attached to Gal in a linear structure (i) (19), or attached to Gal (ii) (20), or attached to GlcNAc (iii) (21) in a branched structure, have been found in mucus glycoproteins in human respiratory systems. The sulfated O-glycan structure was characterized using MS/MS (supplemental Fig. 5N) and the diagnostic fragment ion at 505.1 *m/z* represented a sulfated HexNAc-HexNAc-OH which identified that the particular sulfated structure lost from the glycoproteins of dEpoB300 cells was Gal (β 1-4) [HSO₃(-6)]GlcNAc (β 1-6) [Gal(β 1-3)]GalNAc (iii).

Sialylation Changes on Cell Membrane Glycoproteins—To determine whether the alteration in sialylation associated with acquired resistance to the dEpoB drug occurred to *N*-glycans on a particular cell membrane glycoprotein, we analyzed the *N*-glycan structures on cell membrane glycoproteins separated based on molecular weight. Enriched cell membrane proteins purified by detergent phase partitioning were separated by SDS-PAGE (Fig. 4A), and electroblotted to PVDF membrane. After staining proteins with Direct blue 71, the protein bands were cut out at five molecular weight ranges, approximately <35 kDa, 35–55 kDa, 55–85 kDa, 85–200 kDa, and >200 kDa. *N*-Glycans from the five molecular weight bands were released and analyzed by LC-ESI MS and MS/MS. The EIC of 1184.4 *m/z* [core fucosylated disialo-biantennary *N*-glycan (structure #14)] showed that the major isomer of this *N*-glycan in CEM cells was structure #14b (terminated with one α 2-6 NeuAc and one α 2-3 NeuAc, Fig. 4B) in all five molecular weight bands whereas the major isomeric change to structure #14c (both branches terminated by α 2-3 NeuAc, Fig. 4C) occurred in all molecular weight bands of membrane proteins extracted from CEM/dEpoB300 cells. That is, it is clear that the reduction in α 2-6 NeuAc sialylation has occurred on the *N*-glycans of all, or at least most, of the cell membrane glycoproteins.

Cell Staining with Fluorescently Labeled Lectins—Cell staining with fluorescently labeled lectins was carried out in order to confirm that the decrease of α 2-6 sialylated *N*-glycans in CEM/dEpoB300 cells was not caused by an increase of α 2-3 sialylated *N*-glycans. CEM and CEM/dEpoB300 cells were reacted with biotin conjugated *Sambucus sieboldiana* (SSA) lectin (recognizes α 2-6 sialylated glycans) or biotin conjugated *Maackia amurensis* (MAM) lectin

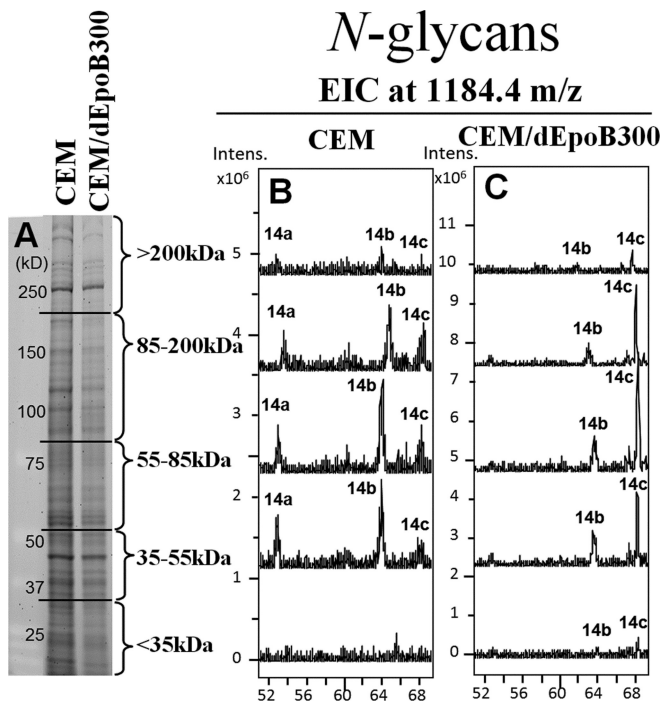


FIG. 4. **N-glycan structures on fractions of cell membrane proteins separated by SDS-PAGE.** A, SDS-PAGE of the total cell membrane proteins from CEM cell and CEM/dEpoB300 cells. EIC of 1184.4 m/z corresponding to fucosylated disialo-bi-antennary *N*-glycan (structure #14) on cell membrane proteins separated into five different molecular weight ranges (<35 kDa, 35–55 kDa, 55–85 kDa, 85–200 kDa and >200 kDa) derived from CEM cell (B) and CEM/dEpoB300 cell (C).

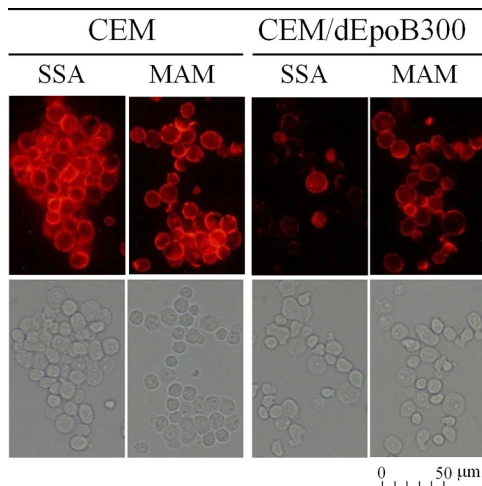


FIG. 5. **Cell staining with fluorescently labeled lectins.** CEM cells and CEM/dEpoB300 cells were stained with PE Cy7-labeled SSA lectin and MAM lectin via biotin-streptavidin binding. SSA lectin and MAM lectin recognize α 2–6 sialic acids and α 2–3 sialic acids, respectively.

(recognize α 2–3 sialylated glycans). The reacted cells were mixed with streptavidin conjugated R-phycoerythrin-cyanine dye (PE-Cy7), and were observed using fluorescence microscopy (Fig. 5). In CEM/dEpoB300 cells, the number of cells

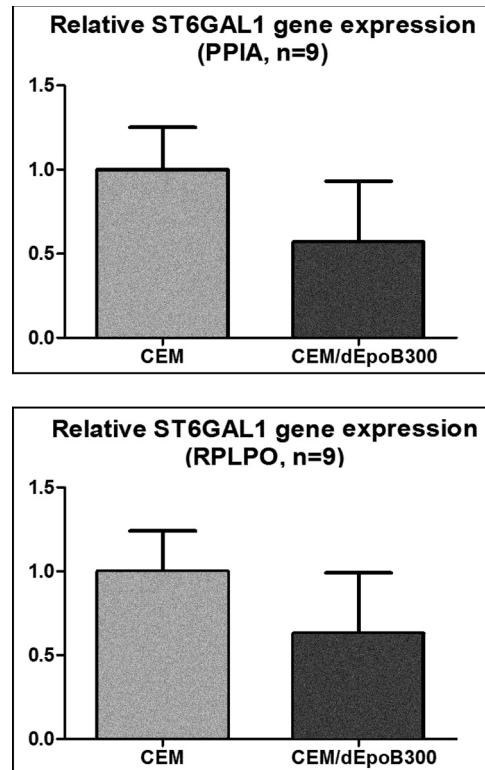


FIG. 6. **Quantitative Real Time RT-PCR of ST6GAL-I.** The relative gene expression of ST6GAL-I in CEM and CEM/dEpoB300 cells were determined using two independent housekeeping genes, human *Cyclophilin A* (*PPIA*) and human *large ribosomal protein* (*RPLPO*). Three individual experiments were performed in triplicate.

recognized with SSA lectin was seen to decrease, but number of cells recognized with MAM lectin did not change when compared with lectin labeled CEM cells. This result showed α 2–6 sialylated *N*-glycans decreased without an apparent increase of α 2–3 sialylated *N*-glycans in the drug resistant CEM/dEpoB300 cells and corroborates the glycan analysis data. This decrease of α 2–6 sialylation on the *N*-glycans of all, or at least most, of the cell membrane glycoproteins may presumably be caused by a decrease of expression and/or activity of the α 2–6 sialyltransferase (ST6Gal), which catalyzes the addition of sialic acids, via a NeuAc α 2–6-Gal linkage, to the terminal Gal of glycoconjugates.

Quantitative Real Time RT-PCR of ST6GAL-I—To test whether there is a decrease in the expression of ST6Gal in the drug resistant CEM/dEpoB300 cells, we determined the relative gene expression of ST6GAL-I in CEM and CEM/dEpoB300 cells by quantitative Real Time RT-PCR (qRT-PCR) using two independent reference housekeeping genes, human *Cyclophilin A* (*PPIA*) and human *large ribosomal protein* (*RPLPO*). The relative gene expression of ST6GAL-I was calculated using the $\Delta\Delta$ CT method. The data represents three individual experiments performed in triplicate (Fig. 6). Consistent with the decrease in α 2–6 sialic acid on the *N*-glycans, there was a measured decrease in expression of ST6GAL-I in

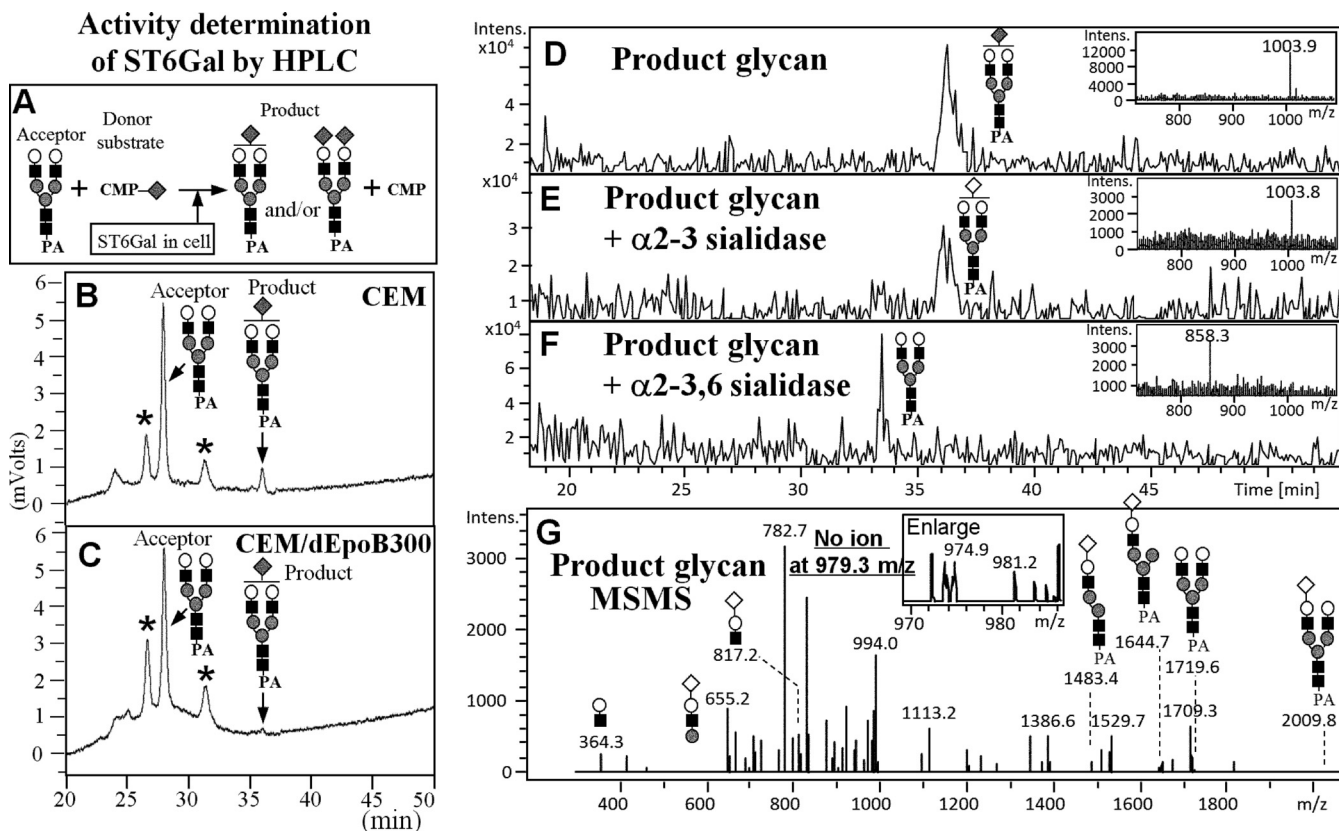


FIG. 7. Determination of the activity of ST6Gal-I enzyme in CEM and CEM/dEpoB300 cells. A–C: HPLC analysis using PA-labeling biantennary glycan as acceptor and CMP-NeuAc as donor substrate. A, Principle of this determination. B and C, HPLC of cell lysate of CEM cells (B) and CEM/dEpoB300 cells (C). Peak at 36.0 min in chromatogram (B) and (C) is the product glycan, and asterisked peaks are derived from cell lysate and are not related to glycans (see supplemental Fig. 7B and C). D–G: MS and MS/MS analysis of the product glycan collected from HPLC separation shown in (B). BPC and mass of the product glycan (D) after treatment with α 2-3 sialidase (E) and α 2-3,6 sialidase (F). G, MS/MS analysis of the peak observed at 36.5 min in (D).

CEM/dEpoB300 cells (43% relative to ST6GAL-I in CEM cells (when used *PPIA* as control gene), and 37% relative to ST6GAL-I in CEM cells (when used *RPLPO* as control gene)), however this did not achieve statistical significance using the unpaired, two tailed *t* test with 95% confidence interval for the nine runs.

Activity of ST6Gal in CEM and CEM/dEpoB Cells—The activity of ST6Gal expressed in CEM cell and CEM/dEpoB cells was tested by HPLC analysis of the conversion of a fluorescently labeled substrate to its α 2-6 sialylated product (Fig. 7A–7C). PA-labeled bi-antennary asialo-*N*-glycan as acceptor, and CMP-NeuAc as donor substrate, were mixed with a cell lysate of CEM (10^7 cells) and CEM/dEpoB300 (10^7 cells). After overnight incubation, the PA-labeled bi-antennary sialo-*N*-glycan product was measured by HPLC with fluorescence detection. In Fig. 7B–7C, the fluorescence peak at retention time 28.0 min is the nonreacted excess acceptor glycan, and the peak at 36.0 min is the product glycan. The peaks marked with an asterisk are derived from the cell lysate and are unrelated to the reaction (see blank sample analysis in supplemental Fig. 7B–C). The results of this assay with cells selected at lower levels of drug resistance CEM/dEpoB60,

CEM/dEpoB140 and CEM/dEpoB300 are shown in supplemental Fig. 7D–H. We found the α 2-6 sialylated product glycan to be synthesized by all cells except the CEM/dEpoB300 cells.

As there is no commercially available PA-labeled monosialo-bi-antennary *N*-glycan standard, with which to compare the retention time, the bi-antennary sialo-*N*-glycan product was collected from the HPLC column (Fig. 7B) and was analyzed by LC-ESI MS and MS/MS to determine the linkage of the NeuAc. The mass of the product glycan at 36.5 min was 1003.9 *m/z* (Fig. 7D), corresponding to the mass of a PA-labeled monosialo-biantennary *N*-glycan. Digestion with α 2-3 sialidase did not change either the retention time or the mass of the product peak (Fig. 7E) whereas digestion with α 2-3,6 sialidase changed the retention and mass of the product peak to that of a PA-labeled asialo-biantennary *N*-glycan (33.5 min, 858.3 *m/z*; Fig. 7F). Thus the product glycan from the assay of ST6Gal-I in Fig. 7B–7C was confirmed to be a PA-labeled α 2-6 NeuAc monosialo-bi-antennary *N*-glycan. Further structural analysis by MS/MS of this product glycan showed that the diagnostic fragment ion of 979.3 *m/z* (diagnostic of the sialylation of the

α 1–6 Man branch of both a reduced or PA-derivatized bi-antennary *N*-glycan; [supplemental Fig. 2](#)) was not observed (Fig. 7G), thus locating the α 2–6 NeuAc on the α 1–3 Man branch of the bi-antennary *N*-glycan. The product glycan in Fig. 7B–7C were thus confirmed to be an α 2–6 sialylated *N*-glycan, which would be produced by ST6Gal-I, and not by β -galactoside α 2–3- sialyltransferase (ST3Gal).

Based on peak area of 1 pmole standard PA-labeled bi-antennary asialo-*N*-glycan acceptor ([supplemental Fig. 7A](#)) the amount of product formed was calculated from the area of the peaks. Using a lysate from the same cell number (10^7 cells), the CEM cell activity resulted in 608 fmol acceptor glycan remaining and 57.6 fmol of mono-sialylated product glycan formed *i.e.* 8.65% yield (Fig. 7B). This compared with the activity of the dEpoB300 cell lysate of 481 fmol remaining substrate and 6.74 fmol product *i.e.* 1.38%, yield (Fig. 7C). Therefore, the ST6Gal-I activity in the dEpoB300 resistant cells was \sim 6 times less than that in the CEM cells.

DISCUSSION

Detailed analysis of the *N*-glycan and *O*-glycan structures on leukemia cell membrane proteins that have acquired resistance to the tubulin-binding antitumor drug dEpoB showed changes to the membrane glycosylation of the cells. Specifically there was a significant decrease of α 2–6 sialylation of the *N*-glycans on all, or at least most, of the cell membrane glycoproteins. We have determined that this change was caused by a decrease in enzyme activity of ST6Gal and was potentially associated with a decrease in expression of ST6GAL-I gene. This decrease of α 2–6 sialylation was not observed on the *O*-glycans because these structures do not contain the ST6Gal-I substrate structure of Gal β 1–4GlcNAc (23). Two homologs of human ST6Gal have been reported, designated ST6Gal-I and ST6Gal-II. ST6Gal-I has been found in Golgi apparatus as a single-pass type II membrane protein and in the body fluid as a secreted protein (24–26). This gene is ubiquitously expressed, as an enzyme composed of 406 amino acids (mass: 46605 Da) with two potential *N*-glycan binding sites (27). Interestingly, this enzyme preferentially adds α 2–6 NeuAc to Gal β 1–4GlcNAc residues on the Man α 1–3Man branch rather than the Man α 1–6Man branch of bi- and tri-antennary *N*-glycans (28, 29), which agrees with the branch position of the α 2–6 NeuAc structures found to be missing in the CEM/dEpoB drug resistant cells in this study. ST6Gal-II is also found in Golgi apparatus as a single-pass type II membrane protein. The sequence encodes a protein of 529 amino acids (mass: 60158 Da) with 48.9% amino acid sequence identity to ST6Gal-I (22). This enzyme is weakly expressed in some tissues, such as small intestine, colon and fetal brain, and has one potential *N*-glycan binding site.

In our previous study that described the development and characterization of the CEM/dEpoB resistant cells (30), we identified two β I-tubulin mutations which are involved in drug binding and microtubule stability. The CEM/dEpoB resistant

sublines did not display increased expression of the multidrug transporters MDR1 or MRP1, nor did they exhibit reduced paclitaxel accumulation (6). Paclitaxel is a hydrophobic agent, whereas dEpoB is hydrophilic and enters cells via a distinct, yet undetermined cell transport mechanism. In this study, we used a detailed analysis of the products of the cellular glycosylation synthesis pathways to find that the resistance to these drugs also results in a decrease in activity of ST6Gal-I. ST6Gal-I is an enzyme that adds a charged sialic acid monosaccharide, in a highly specific α 2–6 linkage, to the terminus of all *N*-glycans, seemingly on all membrane proteins of the cells. We could speculate that the resultant change in overall membrane charge may allow dEpoB300 resistant cells to change the transport of the drug into the cell and escape apoptosis.

We also analyzed the *N*-glycans on the cell membrane proteins of CEM cells resistant to vincristine (3 nM), another tubulin-binding antitumor drug that inhibits assembly of microtubule structures. The vincristine-resistant cells lost almost all sialylation of their *N*-glycans (both α 2–6 NeuAc and α 2–3 NeuAc) ([supplemental Fig. 8A–E](#)). As in the case of epothilone B resistance, this decrease of sialylation was observed on all cell membrane glycoproteins ([supplemental Fig. 8F–K](#)). This suggests that loss of sialylation on the *N*-glycans of membrane proteins may be a general mechanism of acquiring resistance to tubulin-binding antitumor drugs. The role of sialylation in the acquisition of resistance to these drugs is unknown at this stage and will be the subject of further investigation. In therapeutic terms, the connection between a change to such a specific modification on the surface of the cells and the mechanism of this downstream effect of microtubule targeting drugs may offer a route to new interventions to overcome drug resistance.

Acknowledgments—We thank Dr. Shinobu Kitazume (RIKEN, Saitama, Japan) and Prof. Taeko Miyagi (Miyagi Cancer Center Research Institute, Miyagi, Japan) for gifting us antibodies of ST6Gal-I and NUE1, respectively.

* This research was supported by a Cancer Institute of New South Wales Infrastructure Award, Children's Cancer Institute Australia for Medical Research, which is affiliated with the University of New South Wales and the Sydney Children's Hospital and grants from the New South Wales Cancer Council and a National Health and Medical Research Council Senior Fellowship (M. Kavallaris).

** To whom correspondence should be addressed: Bldg E8C Room 307, Department of Chemistry and Biomolecular Sciences, Macquarie University, NSW 2109, Australia. Tel.: +61-2-9850-8176; Fax: +61-2-9850-8313; E-mail: nicki.packer@mq.edu.au.

☒ This article contains [supplemental Figs. S1 to S8](#).

‡‡ Co-senior authors.

REFERENCES

- Lee, F. Y., Borzilleri, R., Fairchild, C. R., Kamath, A., Smykla, R., Kramer, R., and Vite, G. (2008) Preclinical discovery of ixabepilone, a highly active antineoplastic agent. *Cancer Chemother. Pharmacol.* **63**, 157–166
- Bollag, D. M., McQueney, P. A., Zhu, J., Hensens, O., Koupal, L., Liesch, J., Goetz, M., Lazarides, E., and Woods, C. M. (1995) Epothilones, a new

- class of microtubule-stabilizing agents with a taxol-like mechanism of action. *Cancer Res.* **55**, 2325–2333
3. Kowalski, R. J., Giannakakou, P., and Hamel, E. (1997) Activities of the microtubule-stabilizing agents epothilones A and B with purified tubulin and in cells resistant to paclitaxel (Taxol(R)). *J. Biol. Chem.* **272**, 2534–2541
 4. Kavallaris, M. (2010) Microtubules and resistance to tubulin-binding agents. *Nat. Rev. Cancer* **10**, 194–204
 5. Chou, T. C., Zhang, X. G., Balog, A., Su, D. S., Meng, D., Savin, K., Bertino, J. R., and Danishefsky, S. J. (1998) Desoxyepothilone B: an efficacious microtubule-targeted antitumor agent with a promising in vivo profile relative to epothilone B. *Proc. Natl. Acad. Sci. U.S.A.* **95**, 9642–9647
 6. Verrills, N. M., Flemming, C. L., Liu, M., Ivery, M. T., Cobon, G. S., Norris, M. D., Haber, M., and Kavallaris, M. (2003) Microtubule alterations and mutations induced by desoxyepothilone B: implications for drug-target interactions. *Chem. Biol.* **10**, 597–607
 7. Malagolini, N., Chiricolo, M., Marini, M., and Dall'Olio, F. (2009) Exposure of alpha2,6-sialylated lactosaminic chains marks apoptotic and necrotic death in different cell types. *Glycobiology* **19**, 172–181
 8. Honma, K., Iwao-Koizumi, K., Takeshita, F., Yamamoto, Y., Yoshida, T., Nishio, K., Nagahara, S., Kato, K., and Ochiya, T. (2008) RPN2 gene confers docetaxel resistance in breast cancer. *Nat. Med.* **14**, 939–948
 9. Lee, A., Kolarich, D., Haynes, P. A., Jensen, P. H., Baker, M. S., and Packer, N. H. (2009) Rat liver membrane glycoproteome: enrichment by phase partitioning and glycoprotein capture. *J. Proteome Res.* **8**, 770–781
 10. Elortza, F., Nühse, T. S., Foster, L. J., Stensballe, A., Peck, S. C., and Jensen, O. N. (2003) Proteomic analysis of glycosylphosphatidylinositol-anchored membrane proteins. *Mol. Cell. Proteomics* **2**, 1261–1270
 11. Wissing, J., Heim, S., Flohe, L., Bilitewski, U., and Frank, R. (2000) Enrichment of hydrophobic proteins via Triton X-114 phase partitioning and hydroxyapatite column chromatography for mass spectrometry. *Electrophoresis* **21**, 2589–2593
 12. Wilson, N. L., Schulz, B. L., Karlsson, N. G., and Packer, N. H. (2002) Sequential analysis of N- and O-linked glycosylation of 2D-PAGE separated glycoproteins. *J. Proteome Res.* **1**, 521–529
 13. Dall'Olio, F., Malagolini, N., and Chiricolo, M. (2006) Beta-galactoside alpha2,6-sialyltransferase and the sialyl alpha2,6-galactosyl-linkage in tissues and cell lines. *Methods Mol. Biol.* **347**, 157–170
 14. Green, E. D., Adelt, G., Baenziger, J. U., Wilson, S., and Van Halbeek, H. (1988) The asparagine-linked oligosaccharides on bovine fetuin. Structural analysis of N-glycanase-released oligosaccharides by 500-megahertz 1H NMR spectroscopy. *J. Biol. Chem.* **263**, 18253–18268
 15. Townsend, R. R., Hardy, M. R., Cumming, D. A., Carver, J. P., and Bendiak, B. (1989) Separation of branched sialylated oligosaccharides using high-pH anion-exchange chromatography with pulsed amperometric detection. *Anal. Biochem.* **182**, 1–8
 16. Pabst, M., Bondili, J. S., Stadlmann, J., Mach, L., and Altmann, F. (2007) Mass + retention time = structure: a strategy for the analysis of N-glycans by carbon LC-ESI-MS and its application to fibrin N-glycans. *Anal. Chem.* **79**, 5051–5057
 17. Karlsson, N. G., and Packer, N. H. (2002) Analysis of O-linked reducing oligosaccharides released by an in-line flow system. *Anal. Biochem.* **305**, 173–185
 18. Royle, L., Mattu, T. S., Hart, E., Langridge, J. I., Merry, A. H., Murphy, N., Harvey, D. J., Dwek, R. A., and Rudd, P. M. (2002) An analytical and structural database provides a strategy for sequencing O-glycans from microgram quantities of glycoproteins. *Anal. Biochem.* **304**, 70–90
 19. Mawhinney, T. P., Adelstein, E., Morris, D. A., Mawhinney, A. M., and Barbero, G. J. (1987) Structure determination of five sulfated oligosaccharides derived from tracheobronchial mucus glycoproteins. *J. Biol. Chem.* **262**, 2994–3001
 20. Lamblin, G., Rahmoune, H., Wieruszkeski, J. M., Lhermitte, M., Strecker, G., and Roussel, P. (1991) Structure of two sulphated oligosaccharides from respiratory mucins of a patient suffering from cystic fibrosis. A fast-atom-bombardment m.s., and 1H-n.m.r. spectroscopic study. *Biochem. J.* **275 (Pt 1)**, 199–206
 21. Lo-Guidice, J. M., Wieruszkeski, J. M., Lemoine, J., Verbert, A., Roussel, P., and Lamblin, G. (1994) Sialylation and sulfation of the carbohydrate chains in respiratory mucins from a patient with cystic fibrosis. *J. Biol. Chem.* **269**, 18794–18813
 22. Takashima, S., Tsuji, S., and Tsujimoto, M. (2002) Characterization of the second type of human beta-galactoside alpha 2,6-sialyltransferase (ST6Gal II), which sialylates Galbeta 1,4GlcNAc structures on oligosaccharides preferentially. Genomic analysis of human sialyltransferase genes. *J. Biol. Chem.* **277**, 45719–45728
 23. Weinstein, J., de Souza-e-Silva, U., and Paulson, J. C. (1982) Sialylation of glycoprotein oligosaccharides N-linked to asparagine. Enzymatic characterization of a Gal beta 1 to 3(4)GlcNAc alpha 2 to 3 sialyltransferase and a Gal beta 1 to 4GlcNAc alpha 2 to 6 sialyltransferase from rat liver. *J. Biol. Chem.* **257**, 13845–13853
 24. Grundmann, U., Nerlich, C., Rein, T., and Zettlmeissl, G. (1990) Complete cDNA sequence encoding human beta-galactoside alpha-2,6-sialyltransferase. *Nucleic Acids Res.* **18**, 667
 25. Kurosawa, N., Hamamoto, T., Lee, Y. C., Nakaoka, T., Kojima, N., and Tsuji, S. (1994) Molecular cloning and expression of GalNAc alpha 2,6-sialyltransferase. *J. Biol. Chem.* **269**, 1402–1409
 26. Weinstein, J., Lee, E. U., McEntee, K., Lai, P. H., and Paulson, J. C. (1987) Primary structure of beta-galactoside alpha 2,6-sialyltransferase. Conversion of membrane-bound enzyme to soluble forms by cleavage of the NH2-terminal signal anchor. *J. Biol. Chem.* **262**, 17735–17743
 27. Chen, R., Jiang, X., Sun, D., Han, G., Wang, F., Ye, M., Wang, L., and Zou, H. (2009) Glycoproteomics analysis of human liver tissue by combination of multiple enzyme digestion and hydrazide chemistry. *J. Proteome Res.* **8**, 651–661
 28. Joziase, D. H., Schiphorst, W. E., van den Eijnden, D. H., van Kuik, J. A., van Halbeek, H., and Vliegthart, J. F. (1985) Branch specificity of bovine colostrum CMP-sialic acid: N-acetylglucosaminidase alpha 2–6-sialyltransferase. Interaction with biantennary oligosaccharides and glycopeptides of N-glycosylproteins. *J. Biol. Chem.* **260**, 714–719
 29. van den Eijnden, D. H., Joziase, D. H., Dorland, L., van Halbeek, H., Vliegthart, J. F., and Schmid, K. (1980) Specificity in the enzymic transfer of sialic acid to the oligosaccharide branches of b1- and triantennary glycopeptides of alpha 1-acid glycoprotein. *Biochem. Biophys. Res. Commun.* **92**, 839–845
 30. Verrills, N. M., and Kavallaris, M. (2003) Drug resistance mechanisms in cancer cells: a proteomics perspective. *Curr. Opin. Mol. Ther.* **5**, 258–265

In order to cite this article properly, please include all of the following information: Nakano, M., Saldanha, R., Göbel, A., Kavallaris, M., and Packer, N. H. (2011) Identification of Glycan Structure Alterations on Cell Membrane Proteins in Desoxyepothilone B Resistant Leukemia Cells. *Mol. Cell. Proteomics* 10(11): M111.009001. DOI: 10.1074/mcp.M111.009001.